Establishment of a two-phase non-linear simulation model of the dynamic operation of the induction machine

Tarek Kasmieh, Yvan Lefèvre, Xavier Roboam, Jean Faucher

Eur. Phys. J. AP **1**, 57–66 (1998)

THE EUROPEAN PHYSICAL JOURNAL APPLIED PHYSICS

Establishment of a two-phase non-linear simulation model of the dynamic operation of the induction machine*

T. Kasmieh[a], Y. Lefevre, X. Roboam, and J. Faucher

LEEI-UPRES-A[b] 2, rue Charles Camichel, BP 7122, 31071 Toulouse Cedex 7, France

Received: 20 March 1997 / Revised: 22 July 1997 / Accepted: 17 October 1997

Abstract. This paper presents a non-linear model of the induction machine which takes in consideration the influence of the saturation on its behaviour. The approach, based on the Park's two-phase model, is established using a finite-element flux calculation program. This program allows to validate hypothesis formulated in order to simplify flux-current relationships. A comparison between the dynamic response of the model and the response obtained by a general model based on the coupled electro-magnetic equations permits to validate it.

PACS. 02.60.-x Numerical approximation and analysis

1 Introduction

To analyse the behaviour of the induction machine, several approaches are described in the literature. The simulation of the asynchronous motor is mainly performed using the two-phase approach. This approach consists in reducing the machine to a set of simple equivalent coils along two axes in magnetic quadrature and the resulting equations are expressed in terms of the instantaneous coil voltages, currents and rotor speed. This simple model still forms the basis of many drive system control algorithms and predictions because of its general availability and low cost processing.

The complexity of machines actually used demands more accurate modelisation to account for non-linear phenomena such as the magnetic saturation and the frequency effect. Today, the modelisation by the finite-element approach offers a high degree of accuracy [1,6]. Nevertheless, this approach demands a very high calculation time.

The aim of our study is to establish a non-linear model of the asynchronous machine, based on the two-phase approach, which takes in consideration the magnetic saturation. The main purpose of this paper is to introduce the variation of the permeability in flux-current relationships in the two-phase reference. These relationships are determined by using a steady-state finite-element program: *EFCAD* [6]. This program permits to have access to the squirrel cage rotor and to impose directly currents in its bars. Therefore, we can calculate all mutual and self cyclic inductances.

The originality of the proposed approach, with regards to the existant non-linear approaches in the two-phase references [7–9], is that it does not consider any constraint on leakage inductances.

The paper will develop the electro-mechanical equations issued from the determined flux-current relationships. It proposes a method of resolution of the obtained non-linear equation system.

In order to demonstrate the accuracy and the rapidity of the model, we compare the dynamic responses of our approach and of a general model based on the coupled electro-magnetic equations [6].

2 Problem presentation

The saturation of the magnetic material causes a diminution of its permeability, which induces a diminution of the inductances values of the magnetic system. For an induction machine, its magnetic state is defined by the absorbed stator currents and the rotor currents due to the charge. The fact that the inductances in three-phase axes depend on rotor position, their evolution with the currents is relativelly difficult to determine, therefore, we will consider the reduced two-phase model: Park model. Consequently, cyclic inductances are independent of the rotor position.

The two-phase model is obtained using 3 to 2 phases transformation (T_{32}) for the stator, and m to 2 phases transformation (T_{m2}) for the rotor, where m is the number of the phases considered in the rotor which is modelised by the multiphases approach [2,3]. The multiphases approach considers as many phases as bars per pole in the rotor.

The two-phase model is shown in Figure 1.

* This paper was presented at NUMELEC'97.

[a] e-mail: kasmieh@leei.enseeiht.fr

[b] CNRS N 5004

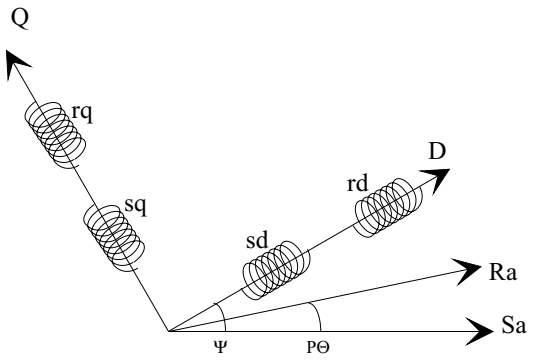

Fig. 1. Two-phase model of the induction machine.

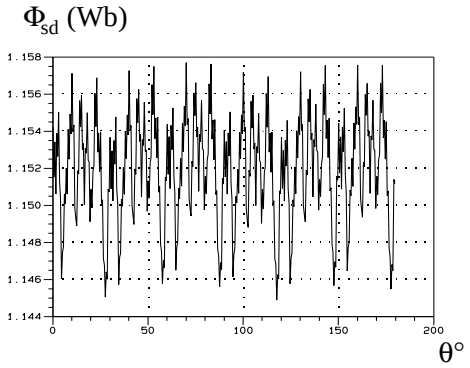

Fig. 3. $\Phi_{\rm sd}$ as a function of rotor position.

In the general case, for the magnetic system of Figure 1, the flux-current relationships are:

$$\begin{aligned}
\Phi_{\rm sd} &= L_{\rm sd}I_{\rm sd} + M_{\rm srd}I_{\rm rd} + \Phi_{\rm dq1}\\
\Phi_{\rm sq} &= L_{\rm sq}I_{\rm sq} + M_{\rm srq}I_{\rm rq} + \Phi_{\rm qd2}\\
\Phi_{\rm rd} &= L_{\rm rd}I_{\rm rd} + M_{\rm rsd}I_{\rm sd} + \Phi_{\rm dq2}\\
\Phi_{\rm rq} &= L_{\rm rq}I_{\rm rq} + M_{\rm rsq}I_{\rm sq} + \Phi_{\rm qd2}
\end{aligned} \tag{1}$$

with:

$$\begin{aligned}
\Phi_{\rm dq1} &= M_{\rm ssdq}I_{\rm sd} + M_{\rm srdq}I_{\rm rq}\\
\Phi_{\rm qd1} &= M_{\rm ssqd}I_{\rm sd} + M_{\rm srqd}I_{\rm rd}\\
\Phi_{\rm dq2} &= M_{\rm rrdq}I_{\rm rd} + M_{\rm srdq}I_{\rm sq}\\
\Phi_{\rm qd2} &= M_{\rm rrqd}I_{\rm rd} + M_{\rm rsqd}I_{\rm sd}
\end{aligned} \tag{2}$$

where self and mutual cyclic inductances are functions of ($I_{\rm sd}$, $I_{\rm sq}$, $I_{\rm rd}$, $I_{\rm rq}$).

The fluxes $\Phi_{{\rm dq}x}$ and $\Phi_{{\rm qd}x}$ are the fluxes on the **D** and **Q** axes due to the **Q** and **D** currents.

In Section 3, we will use a finite element program to simplify flux-current relationships under saturation conditions. Then we will determine, by introducing the permeability variation, the evolution of cyclic inductances with the stator and the rotor currents.

The study presented in this paper is based on the following assumption.

1 - Only the first harmonic of the fluxes is taken into account.

2 - The magnetic system of Figure 1 is symmetrical and balanced.

The approach is verified on two squirrel cage induction machines of 4 poles and of 4 kW and 45 kW.

3 Determination of flux-current relationships using the $EFCAD$ program under saturation conditions

To establish flux-current relationships we use the modulus $EFCR$ of $EFCAD$ program. This modulus permits to take into account saturation curve of the magnetic materials and to calculate the flux and the torque as functions of the rotor position for imposed values of the stator and the rotor currents [6].

Figure 2 shows the calculation procedure of the fluxes ($\Phi_{\rm sd}$, $\Phi_{\rm sq}$, $\Phi_{\rm rd}$, $\Phi_{\rm rq}$). A first modulus permits to calculate, by means of the inversed park transformation (T_{32}^{-1}), the currents in the stator coils and in the bars of the cage from imposed values of the Park's currents components ($I_{\rm sd}$, $I_{\rm sq}$, $I_{\rm rd}$, $I_{\rm rq}$). Then, the modulus $EFCR$ calculates the fluxes in the stator coils and in the cage bars as functions of the rotor position. Finally, we calculate the fluxes in the two-axes reference using Park's transformations, so, only the first harmonic of the fluxes is accounted.

Later we will make reference to this calculation procedure as the procedure P1, Figure 2.

As it is shown in Figure 2, the final calculated values of the fluxes are the average values with regards to the rotor position. In fact, in order to neglect the influence of slots, we will calculate the fluxes for several positions of the rotor for the same current vector, then we will take the DC level.

To illustrate the idea of the procedure P1, Figure 3 shows the stator **D** flux calculated for several positions of the rotor for the same current vector (100, 0, 0,0).

$$\begin{bmatrix} I_{\rm sd}(\theta)\\ I_{\rm sq}(\theta)\\ I_{\rm rd}(\theta)\\ I_{\rm rq}(\theta)\end{bmatrix} \underset{[T_{m2}]^{-1}}{\overset{[T_{32}]^{-1}}{\rightarrow}} \begin{bmatrix}[I_s(\theta)]\\ [I_r(\theta)]\end{bmatrix} \overrightarrow{EFCR} \begin{bmatrix}[\Phi_s(\theta)]\\ [\Phi_r(\theta)]\end{bmatrix} \underset{[T_{m2}]}{\overset{[T_{32}]}{\rightarrow}} \begin{bmatrix} <\Phi_{\rm sd}(\theta)>=\Phi_{\rm sd}\\ <\Phi_{\rm sq}(\theta)>=\Phi_{\rm sq}\\ <\Phi_{\rm sq}(\theta)>=\Phi_{\rm sq}\\ <\Phi_{\rm rq}(\theta)>=\Phi_{\rm rq}\end{bmatrix}^{(*)}$$

Fig. 2. Calculation procedure of the fluxes: P1, *: $< x(\theta) >$ is the average value of x.

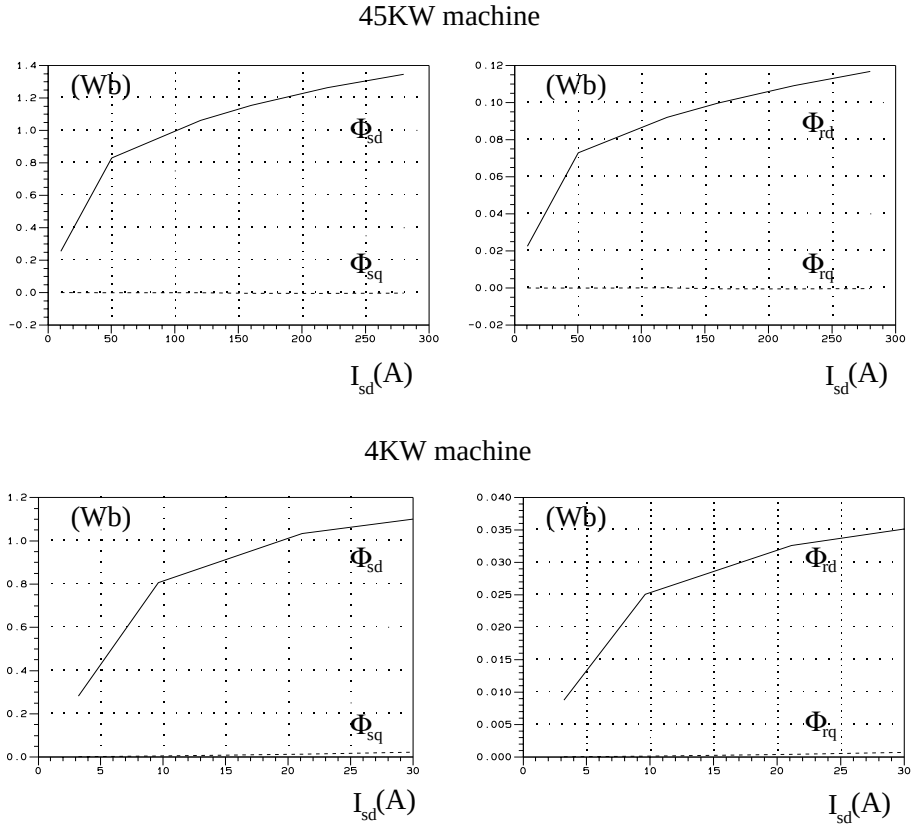

Fig. 4. Fluxes evolution with I_{sd}.

3.1 Simplification of flux-current relationships

Theoretically, for the magnetic system of Figure 1, the fluxes $\Phi_{\mathrm{dq}x}$ and $\Phi_{\mathrm{qd}x}$ are null because the axes **D** and **Q** are perpendicular. To validate this hypothesis under saturation conditions, we impose only one current I_{sd} and calculate the fluxes (Φ_{sd}, Φ_{sq}, Φ_{rd}, Φ_{rq}). The maximum value taken for I_{sd} is three times the nominal current I_{nom} for each machine. Evolutions of the fluxes with I_{sd} are shown in Figure 4.

We find that the maximum ratio of the flux on the **Q** axis and the flux on the **D** axis for the same armature is for the maximum value of I_{sd}:

$$\frac{\Phi_{\mathrm{q}x}}{\Phi_{\mathrm{d}x}} = 0.76\% \text{ for 4 kW motor,}$$

$$\frac{\Phi_{\mathrm{q}x}}{\Phi_{\mathrm{d}x}} = 0.30\% \text{ for 45 kW motor.}$$

Depending on these results, we can write the following simplified flux-current relationships:

$$\begin{aligned} \Phi_{\mathrm{s}x} &= L_{\mathrm{s}x} I_{\mathrm{s}x} + M_{\mathrm{sr}x} I_{\mathrm{r}x}, \\ \Phi_{\mathrm{r}x} &= L_{\mathrm{r}x} I_{\mathrm{r}x} + M_{\mathrm{rs}x} I_{\mathrm{s}x}. \end{aligned} \tag{3}$$

Where x is put for **D** and **Q**.

3.2 Cyclic inductances evolution with the magnetic state of the machine

From the equation (3) we can calculate self and mutual cyclic inductances by applying the procedure P1:

$$\begin{aligned} L_{\mathrm{sd}}(I_{\mathrm{sd}}) &= \frac{\Phi_{\mathrm{sd}}}{I_{\mathrm{sd}}} \text{ for } I_{\mathrm{sq}} = I_{\mathrm{rd}} = I_{\mathrm{rq}} = 0, \\ M_{\mathrm{rsd}}(I_{\mathrm{sd}}) &= \frac{\Phi_{\mathrm{rd}}}{I_{\mathrm{sd}}} \text{ for } I_{\mathrm{sq}} = I_{\mathrm{rd}} = I_{\mathrm{rq}} = 0, \\ L_{\mathrm{rd}}(I_{\mathrm{rd}}) &= \frac{\Phi_{\mathrm{rd}}}{I_{\mathrm{rd}}} \text{ for } I_{\mathrm{sd}} = I_{\mathrm{sq}} = I_{\mathrm{rq}} = 0, \\ M_{\mathrm{srd}}(I_{\mathrm{rd}}) &= \frac{\Phi_{\mathrm{sd}}}{I_{\mathrm{rd}}} \text{ for } I_{\mathrm{sd}} = I_{\mathrm{sq}} = I_{\mathrm{rq}} = 0. \end{aligned}$$

Figures 5 and 6 show cyclic mutual and self inductances evolution with the specified currents.

The same curves are obtained for the inductances on the **Q** axis because of the symmetry of the machine.

We remark, for the cyclic mutual inductances, that there are values of $I_{\mathrm{sd}} = I_{\mathrm{sd}\alpha}$ and $I_{\mathrm{rd}} = I_{\mathrm{rd}\alpha}$ which verify:

$$M_{\mathrm{srd}}(I_{\mathrm{rd}\alpha}) = M_{\mathrm{rsd}}(I_{\mathrm{sd}\alpha}). \tag{4}$$

In fact, the ratio $\alpha = I_{\mathrm{sd}\alpha}/I_{\mathrm{rd}\alpha}$ defines the reference factor of the machine. Figure 7 shows the evolution of $I_{\mathrm{sd}\alpha}$ as a function of $I_{\mathrm{rd}\alpha}$. We notice that, effectively, the curves obtained are straight lines with slopes:

$$\alpha_{45 \text{ kW machine}} = 0.087, \ \alpha_{45 \text{ kW machine}} = 0.02.$$

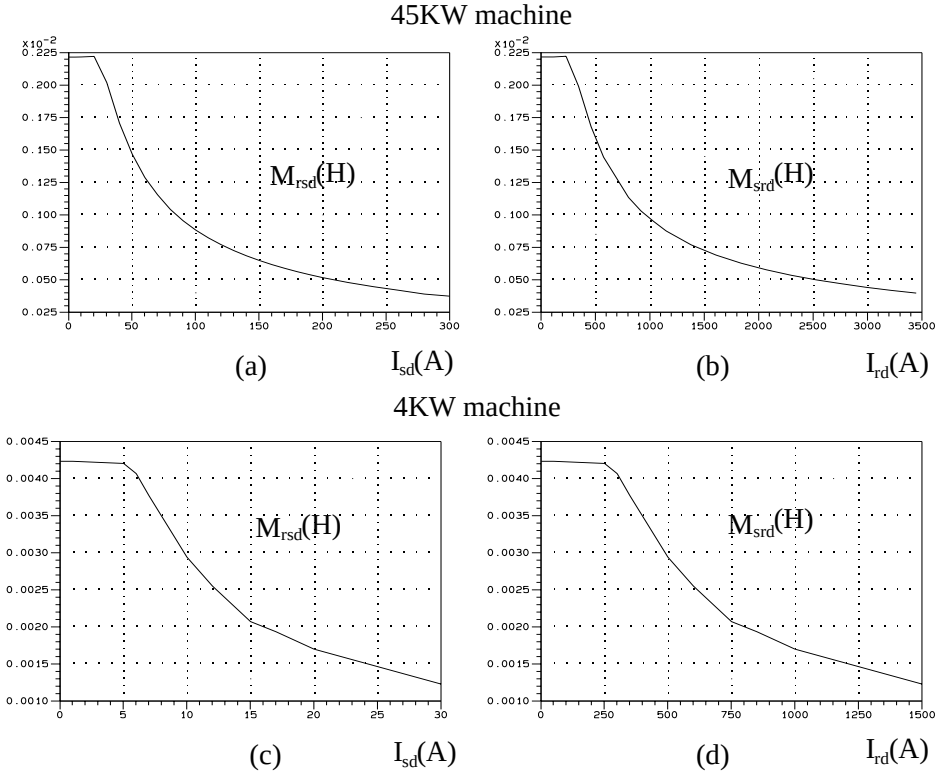

Fig. 5. Mutual inductances evolution obtained for two induction machines: $M_{\mathrm{srd}}((I_{\mathrm{sd}}, 0, 0, 0))$ and $M_{\mathrm{rsd}}((0, 0, I_{\mathrm{rd}}, 0))$.

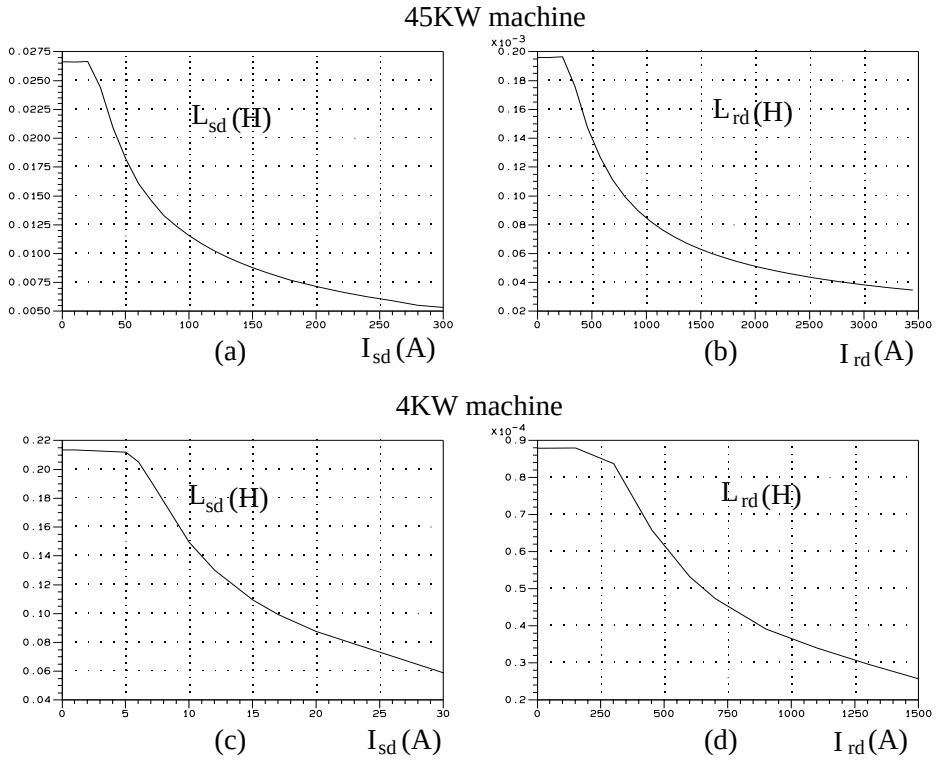

Fig. 6. Self inductances evolution obtained for two induction machines: $L_{\mathrm{sd}}((I_{\mathrm{sd}}, 0, 0, 0))$ and $L_{\mathrm{rd}}((0, 0, I_{\mathrm{rd}}, 0))$.

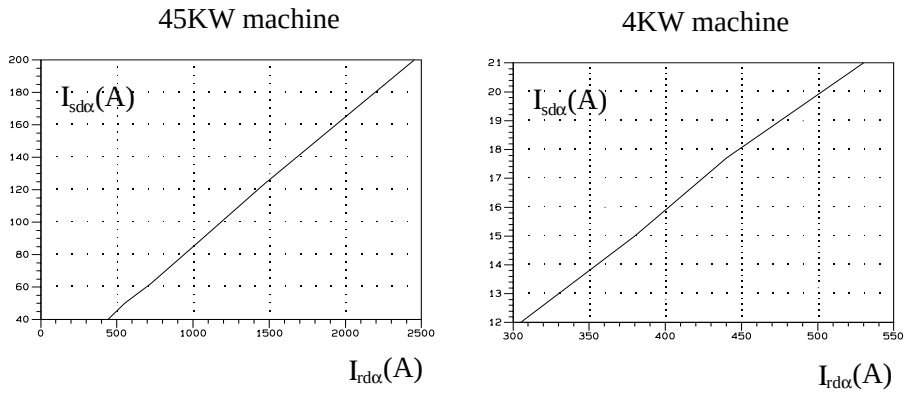

Fig. 7. $I_{\mathrm{sd}\alpha}(I_{\mathrm{rd}\alpha})$.

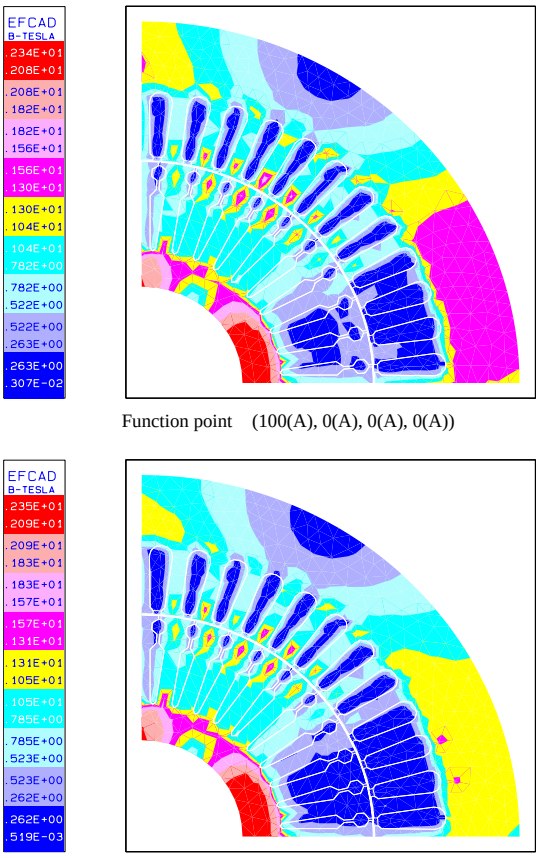

Fig. 8. Magnetic states of the 45 kW machine.

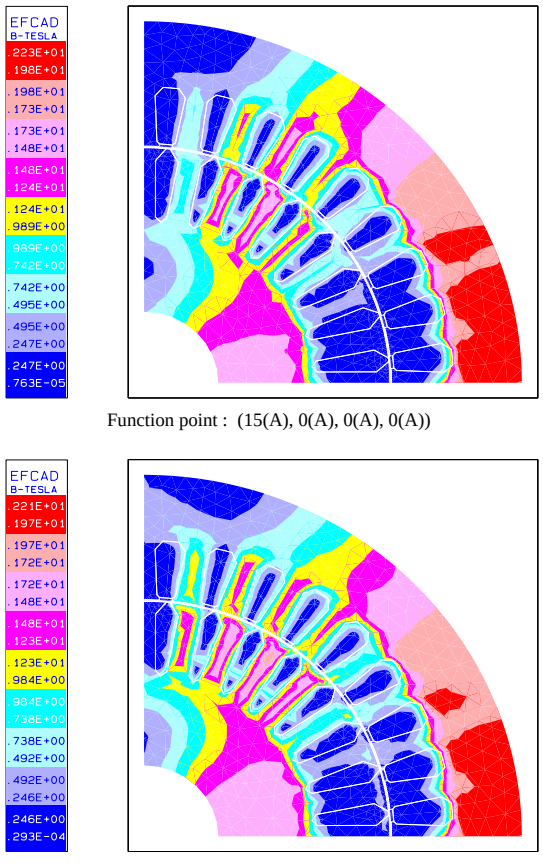

Fig. 9. Magnetic states of the 4 kW machine.

Figures 8 and 9 show that the magnetic states of the machines for the two function points: (I_{sd}, 0, 0, 0) and (0, 0, αI_{sd}, 0) are the same where $I_{\mathrm{sd}} = 100$ (A) for the machine of 45 kW, and $I_{\mathrm{sd}} = 15$ (A) for the machine of 4 kW. This result is consistent with the theory: reference factor depends only on the windings turns number and the phases number in the stator and in the rotor.

3.3 Calculation of the fluxes ($\boldsymbol{\Phi_{\mathrm{sd}}}$, $\boldsymbol{\Phi_{\mathrm{sq}}}$, $\boldsymbol{\Phi_{\mathrm{rd}}}$, $\boldsymbol{\Phi_{\mathrm{rq}}}$) for a functioning point ($\boldsymbol{I_{\mathrm{sd}}}$, $\boldsymbol{I_{\mathrm{sq}}}$, $\boldsymbol{I_{\mathrm{rd}}}$, $\boldsymbol{I_{\mathrm{rq}}}$)

3.3.1 Influence of one-axis currents (**D** or **Q**)

We supply the machine of 45 kW by only currents in the **D** axis I_{sd} and I_{rd}. Using procedure P1 we calculate fluxes for the currents (I_{sd}, 0, I_{rd}, 0), so we obtain the points a_{is} and a_{ir}; $i = 1, 2$: Figure 10. We do this experiment for several values of I_{sd} and I_{rd} which give the same magnetic

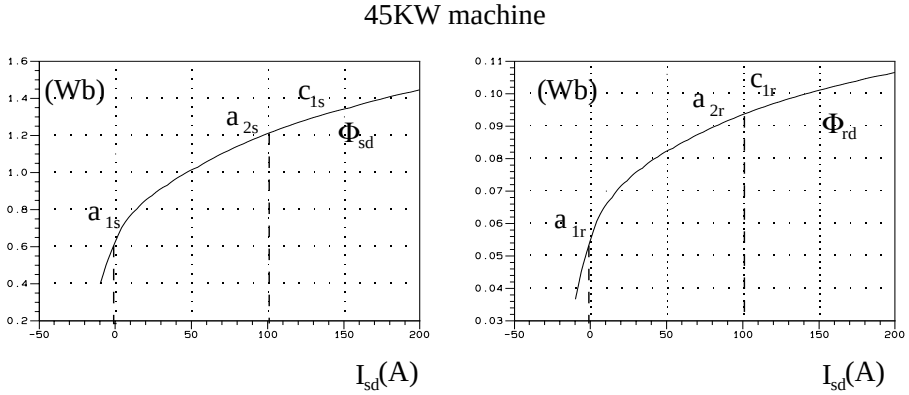

Fig. 10. Stator flux $\Phi_{\rm sd}$ and rotor flux $\Phi_{\rm rd}$ in function of $I_{\rm sd}$: points a_{1s} and a_{1r} are obtained from procedure P1 for a set of currents ($I_{\rm sd}$, $I_{\rm sq}$, $I_{\rm rd}$, $I_{\rm rq}$) equals to (0 (A), 0 (A), 300 (A), 0 (A)) $\Rightarrow$ $\mid I_{\rm m} \mid = 26.11$ (A); points $\rm a_{2s}$ and $\rm a_{2r}$ are obtained from procedure P1 for a set of currents ($I_{\rm sd}$, $I_{\rm sq}$, $I_{\rm rd}$, $I_{\rm rq}$) equals to (100 (A), 0 (A), 300 (A), 0 (A)) $\Rightarrow$ $\mid I_{\rm m} \mid = 126.11$ (A); curves $c_{1\rm s}$ and $c_{1\rm r}$ are obtained from equation (5) for $I_{\rm sq} = I_{\rm rq}$=0 (A) and $I_{\rm rd} = 300$ (A).

Table 1. Dispersion of points $\rm a_1$ et $\rm a_2$ for the specified currents.

Points $\rm a_1$ $\mid I_{\rm m} \mid$=26.11 (A)			
$I_{\rm sd}$ (A)	$I_{\rm rd}$ (A)	$\Phi_{\rm sd}$ (Wb)	$\Phi_{\rm rd}$ (Wb)
10	185.17	0.652	0.0562
20	70.23	0.665	0.0561
0	300	0.666	0.0561

Points $\rm a_2$ $\mid I_{\rm m} \mid$=126.11 (A)			
$I_{\rm sd}$ (A)	$I_{\rm rd}$ (A)	$\Phi_{\rm sd}$ (Wb)	$\Phi_{\rm rd}$ (Wb)
50	874.83	1.149	0.0937
80	530	1.159	0.0938
100	300	1.150	0.0937

D current $I_{\rm md} = I_{\rm sd} + \alpha I_{\rm rd}$. The simulation results show that the points $\rm a_{is}$ and $\rm a_{ir}$ stay fixed, see Table 1.

Now, if we substitute the x-axis currents for cyclic inductance curves in Figures 5a, 6a and 6b, calculated in the previous section, by the current $I_{\rm md} = I_{\rm sd} + \alpha I_{\rm rd}$, we obtain the following relations between the fluxes and the currents in the **D** axis:

$$\begin{aligned} \Phi_{\rm sd} &= L_{\rm sd}(I_{\rm md})I_{\rm sd} + M_d(I_{\rm md})I_{\rm rd}, \\ \Phi_{\rm rd} &= L_{\rm rd}(I_{\rm md})I_{\rm rd} + M_d(I_{\rm md})I_{\rm sd}. \end{aligned} \quad (5)$$

We suppose that $M_{\rm d}(I_{\rm md}) = M_{\rm rsd}(I_{\rm md}) = M_{\rm srd}(I_{\rm md})$.

For the same value of the current $I_{\rm rd}$ taken for the points $\rm a_{is}$ and $\rm a_{ir}$: $I_{\rm rd} = 300$ (A), we trace the fluxes in function of $I_{\rm sd}$ using the equation (5). We notice that the obtained flux curves $c_{1\rm s}$ and $c_{1\rm r}$ lay on the points $\rm a_{is}$ and $\rm a_{ir}$: see Figure 10. This simulation validates the supposed flux-current relationships on the **D** axis for the function point ($I_{\rm sd}$, 0, $I_{\rm rd}$, 0).

As the machine is supposed symmetrical we can write:

$$\begin{aligned} \Phi_{\rm sq} &= L_{\rm sq}(I_{\rm mq})I_{\rm sq} + M_{\rm q}(I_{\rm mq})I_{\rm rq} \\ \Phi_{\rm rq} &= L_{\rm rq}(I_{\rm mq})I_{\rm rq} + M_{\rm q}(I_{\rm mq})I_{\rm sq} \end{aligned} \quad (6)$$

for the currents (0, $I_{\rm sq}$, 0, $I_{\rm rq}$) where $I_{\rm mq} = I_{\rm sq} + \alpha I_{\rm rq}$.

3.3.2 Saturation cross effect

For the same values of currents on the **D** axis taken for the points $\rm a_{is}$ and $\rm a_{ir}$ and using the procedure P1, we supply the machine by the currents on the **Q** axis. We notice that the values of the fluxes decrease: points $\rm b_{is}$ and $\rm b_{ir}$; $i = 1, 2$; see Figure 11. This demonstrates that there is a cross effect between the two axes, **D** and **Q**, due to the saturation. For several experiments, and for different values of $I_{\rm sq}$ and $I_{\rm rq}$ which verify $I_{\rm mq} = I_{\rm sq} + \alpha I_{\rm rq} = 50$ (A), we notice that the points $\rm b_{is}$ and $\rm b_{ir}$ stay fixed.

Now, if we substitute the x-axis currents by the modulus of the magnetizing current for the cyclic inductances we obtain the following supposed flux-current relationships:

$$\begin{aligned} \Phi_{\rm sd} &= L_{\rm sd}(\mid I_{\rm m} \mid)I_{\rm sd} + M_{\rm d}(\mid I_{\rm m} \mid)I_{\rm rd} \\ \Phi_{\rm rd} &= L_{\rm rd}(\mid I_{\rm m} \mid)I_{\rm rd} + M_{\rm d}(\mid I_{\rm m} \mid)I_{\rm sd} \end{aligned} \quad (7)$$

where $\mid I_{\rm m} \mid = \sqrt{I_{\rm md}^2 + I_{\rm mq}^2}$.

For the currents $I_{\rm sq}$, $I_{\rm rd}$ and $I_{\rm rq}$ which define the points b_{is} and b_{ir}, and using equation (7) we trace $\Phi_{\rm sd}$ and $\Phi_{\rm rd}$ in function of $I_{\rm sd}$. We notice that the obtained curves lay on the points $\rm b_{is}$ and $\rm b_{ir}$: see Figure 11.

Therefore, we validate the relationships of the equation (7).

Finally, depending on these experiments and considering the symmetry of the motor, the flux-current relationships are reduced to the following equation:

$$[\Phi] = [M]\,(\mid I_{\rm m} \mid)\,[I] \quad (8)$$

where $[\Phi] = \begin{bmatrix} \Phi_{\rm sd} \\ \Phi_{\rm sq} \\ \Phi_{\rm rd} \\ \Phi_{\rm rq} \end{bmatrix}$, $[I] = \begin{bmatrix} I_{\rm sd} \\ I_{\rm sq} \\ I_{\rm rd} \\ I_{\rm rq} \end{bmatrix}$

and $[M]\,(\mid I_{\rm m} \mid) = \begin{bmatrix} L_{\rm s} & 0 & M & 0 \\ 0 & L_{\rm s} & 0 & M \\ M & 0 & L_{\rm r} & 0 \\ 0 & M & 0 & L_{\rm r} \end{bmatrix} (\mid I_{\rm m} \mid)$.

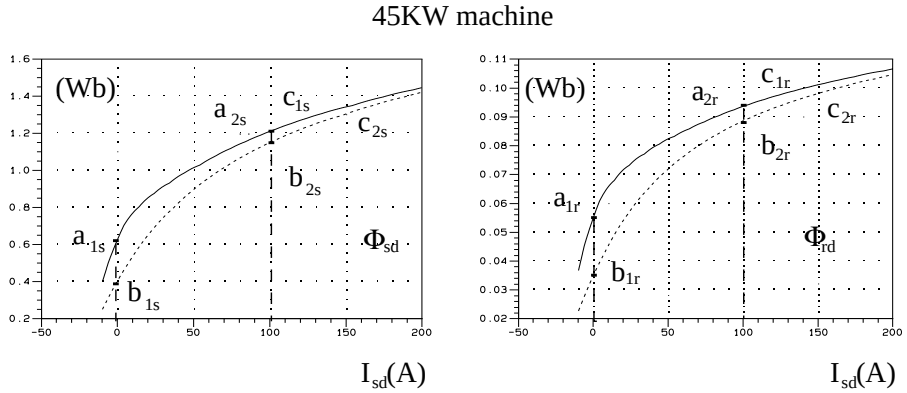

Fig. 11. Stator flux $\Phi_{\rm sd}$ and rotor flux $\Phi_{\rm rd}$ in function of $I_{\rm sd}$ *EFCAD*: points a_{1s} and a_{1r} for the currents (0 (A), 0 (A), 300 (A), 0 (A)); points a_{2s} and a_{2r} for the currents (100 (A), 0 (A), 300 (A), 0 (A)); points b_{1s} and b_{1r} for the currents (0 (A), $I_{\rm sq}$, 300 (A), $I_{\rm rq}$) with $I_{\rm mq}$=50 (A); points b_{2s} and b_{2r} for the currents (100 (A), $I_{\rm sq}$, 300 (A), $I_{\rm rq}$) with $I_{\rm mq}$=50 (A); equation (7): curves c_{1s} and c_{1r} for $I_{\rm sq} = I_{\rm rq} = 0$ and $I_{\rm rd} = 300$ (A), curves c_{2s} and c_{2r} for $I_{\rm mq}$ =50 (A) and $I_{\rm rd}$=300 (A).

$$\begin{bmatrix} I_{\rm sd} \\ I_{\rm sq} \\ I_{\rm rd} \\ I_{\rm rq} \end{bmatrix} - |\, I_m \,| \rightarrow \begin{bmatrix} \text{cyclic} \\ \text{inductances} \\ \text{table} \end{bmatrix} \begin{matrix} \rightarrow L_s(|\, I_m \,|) \\ \rightarrow L_r(|\, I_m \,|) \\ \rightarrow M(|\, I_m \,|) \end{matrix} \rightarrow [\Phi] = [M]\,(|\, I_m \,|)\,[I] \rightarrow \begin{bmatrix} \Phi_{\rm sd} \\ \Phi_{\rm sq} \\ \Phi_{\rm rd} \\ \Phi_{\rm rq} \end{bmatrix}$$

Fig. 12. Procedure 2: P2.

From the equation (8) we can construct a calculation procedure of the fluxes for a function point: ($I_{\rm sd}$, $I_{\rm sq}$, $I_{\rm rd}$, $I_{\rm rq}$). This procedure is shown in Figure 12, and called, in opposition of the first procedure P1, procedure P2.

Table 2 shows some simulation results obtained by the two procedures for the two machines.

We note that the maximum difference calculated between the two results is of 5% for the motor torque and of 2% for the fluxes.

In this section, we demonstrate that there is a symetrical cross-effect due to the saturation of magnetic material for the induction machine. This means that the **D** and **Q** inductances have the same values for a defined magnetic state. In fact, the cross-effect also appears for the synchronous machine, and there is also an influence of an axis current over the inductances of the other axis when the machine is saturated, but for the salient-poles machine this cross-effect is assymetrical and the **D** and **Q** inductances have different values.

4 Electro-mechanical equations

In the two-phases reference, the electrical equations of the machine are:

$$\begin{aligned} v_{\rm sd} &= {\rm R_s} I_{\rm sd} + \frac{{\rm d}\Phi_{\rm sd}}{{\rm d}t} - \frac{{\rm d}\Psi}{{\rm d}t}\Phi_{\rm sq}, \\ v_{\rm sq} &= {\rm R_s} I_{\rm sd} + \frac{{\rm d}\Phi_{\rm sq}}{{\rm d}t} + \frac{{\rm d}\Psi}{{\rm d}t}\Phi_{\rm sd}, \\ v_{\rm rd} &= {\rm R_r} I_{\rm rd} + \frac{{\rm d}\Phi_{\rm rd}}{{\rm d}t} - \frac{{\rm d}(\Psi - p\theta)}{{\rm d}t}\Phi_{\rm rq}, \end{aligned}$$

$$v_{\rm rq} = {\rm R_r} I_{\rm rq} + \frac{{\rm d}\Phi_{\rm rq}}{{\rm d}t} + \frac{{\rm d}(\Psi - p\theta)}{{\rm d}t}\Phi_{\rm rd}. \qquad (9)$$

If we add the validated flux-current relationships (Eq. (8)) we obtain the following non-linear equation system:

$$\left[\frac{{\rm d}\Phi}{{\rm d}t}\right] + [K_{\rm nl}]\,(|\, I_{\rm m} \,|)\,[\Phi] = [V] \qquad (10)$$

where: $[I] = \begin{bmatrix} I_{\rm sd} \\ I_{\rm sq} \\ I_{\rm rd} \\ I_{\rm rq} \end{bmatrix}$, $[V] = \begin{bmatrix} v_{\rm sd} \\ v_{\rm sq} \\ v_{\rm rd} \\ v_{\rm rq} \end{bmatrix}$,

$[\Phi] = \begin{bmatrix} \Phi_{\rm sd} \\ \Phi_{\rm sq} \\ \Phi_{\rm rd} \\ \Phi_{\rm rq} \end{bmatrix}$, $\left[\frac{{\rm d}\Phi}{{\rm d}t}\right] = \begin{bmatrix} \frac{{\rm d}\Phi_{\rm sd}}{{\rm d}t} \\ \frac{d\Phi_{\rm sq}}{{\rm d}t} \\ \frac{{\rm d}\Phi_{\rm rd}}{{\rm d}t} \\ \frac{d\Phi_{\rm rq}}{{\rm d}t} \end{bmatrix}$

and

$[K_{\rm nl}]\,(|\, I_{\rm m} \,|) =$

$$\begin{bmatrix} \frac{{\rm R_s}}{\sigma L_{\rm s}} & -\frac{d\Psi}{{\rm d}t} & -\frac{MR_{\rm s}}{\sigma L_{\rm s} L_{\rm r}} & 0 \\ \frac{{\rm d}\Psi}{{\rm d}t} & \frac{R_{\rm s}}{\sigma L_{\rm s}} & 0 & -\frac{MR_{\rm s}}{\sigma L_{\rm s} L_{\rm r}} \\ -\frac{MR_{\rm s}}{\sigma L_{\rm s} L_{\rm r}} & 0 & \frac{R_{\rm r}}{\sigma L_{\rm r}} & -\frac{d(\Psi - p\theta)}{{\rm d}t} \\ 0 & -\frac{MR_{\rm s}}{\sigma L_{\rm s} L_{\rm r}} & \frac{d(\Psi - p\theta)}{{\rm d}t} & \frac{R_{\rm r}}{\sigma L_{\rm r}} \end{bmatrix} (|\, I_{\rm m} \,|).$$

Table 2. Simulation results with procedures P1 and P2.

4 kW machine, $\mid I_{\mathrm{m}} \mid$=10 (A) I_{sd}=3 (A), I_{sq}=5 (A) I_{rd}=124 (A), I_{rq}=168.4 (A)		
	P1	P2
Φ_{sd} (Wb)	0.820	0.812
Φ_{sq} (Wb)	1.270	1.245
Φ_{rd} (Wb)	0.017	0.016
Φ_{rq} (Wb)	0.026	0.025
c_{em}(nm)	0.640	0.676

4 kW machine, $\mid I_{\mathrm{m}} \mid$=20(A) I_{sd}=5 (A), I_{sq}=12 (A) I_{rd}=250 (A), I_{rq}=266 (A)		
	P1	P2
Φ_{sd} (Wb)	0.897	0.862
Φ_{sq} (Wb)	1.540	1.500
Φ_{rd} (Wb)	0.018	0.016
Φ_{rq} (Wb)	0.031	0.030
c_{em} (nm)	5.850	5.678

45 kW machine, $\mid I_{\mathrm{m}} \mid$=141.79 (A) I_{sd}=100 (A), I_{sq}=30 (A) I_{rd}=300 (A), I_{rq}=400 (A)		
	P1	P2
Φ_{sd} (Wb)	1.123	1.115
Φ_{sq} (Wb)	0.543	0.545
Φ_{rd} (Wb)	0.086	0.086
Φ_{rq} (Wb)	0.044	0.044
c_{em} (nm)	-42.080	-42.200

45 kW machine, $\mid I_{m} \mid$=108.7 (A) I_{sd}=3 (A), I_{sq}=100 (A) I_{rd}=1000 (A), I_{rq}=100 (A)		
	P1	P2
Φ_{sd} (Wb)	0.709	0.708
Φ_{sq} (Wb)	0.993	0.982
Φ_{rd} (Wb)	0.061	0.061
Φ_{rq} (Wb)	0.074	0.074
c_{em} (nm)	138.080	135.790

$[K_{\mathrm{nl}}]\,(\mid I_{\mathrm{m}} \mid)$ is a non-linear matrix which depends on the modulus of the magnetizing current $\mid I_{\mathrm{m}} \mid$ and σ is the dispersion factor.

To describe the electro-mechanical behaviour of the machine we add the mechanical equation:

$$J\frac{\mathrm{d}\Omega}{\mathrm{d}t} = c_{\mathrm{em}} - c_{\mathrm{r}} - f\Omega \tag{11}$$

where c_{em} is the motor torque, its expression (Eq. (12)) stays the same as in the linear case [5]:

$$c_{\mathrm{em}} = p(\Phi_{\mathrm{sd}} I_{\mathrm{sq}} - \Phi_{\mathrm{sq}} I_{\mathrm{sd}}). \tag{12}$$

5 Resolution of the electro-mechanical equations

To solve the non-linear electro-mechanical equations issued from the validated flux-current relationships, we adopt the method of Euler semi-implicite [4].

We write the equation (10) as follows:

$$\left[\frac{\mathrm{d}\Phi}{\mathrm{d}t}\right] = [F([\Phi]_t, [I]_t)] = [F]_t \tag{13}$$

where $[F]$ is the derivative function of $[\Phi]$.

The Euler semi-implicite method consists of calculating the derivative function at the instant $t + \alpha\Delta t$ $(0 \leq \alpha \leq 1)$ where $[F]_{t+\alpha\Delta t} = \alpha\,[F]_{t+\Delta t} + (1-\alpha)\,[F]_t$.

If we develop the equation (10), we obtain the non-linear system:

$$[H]_{t+\Delta t}\,[\Phi]_{t+\Delta t} = [G]_{t+\Delta t} \tag{14}$$

where:

$$\begin{aligned}[H]_{t+\Delta t} &= Id_{4*4} + \alpha\Delta t\,[K_{\mathrm{nl}}]\,,\\ [G]_{t+\Delta t} &= [\Phi]_t + \Delta t\left[\alpha\,[V]_{t+\Delta t}\right.\\ &\quad \left.+(1-\alpha)\,[[V]_t - [K_{\mathrm{nl}}]_t\,[\Phi]]\right].\end{aligned}$$

The algorithm idea is to find a fluxes approximate solution for a fixed precision. The solution research is done by a sequence of iterations using one of the non-linear resolution methods (substitution or Newton-Raphson) [4]. For each iteration of the fluxes calculation loop, we do an another iterations sequence to find the corresponding currents.

The detailed resolution algorithm is shown in Figure 13.

6 Dynamic response

Figure 14 shows the dynamic response of our model and the dynamic response of a general model based on the coupled electro-magnetic equations.

In order to have an important saturation level of the machines, we choose the ratio V/w_{s} bigger than the nominal value of the flux. The diminution of the inductances values is of 53% for the 45 kW machine and of 11% for the 4 kW machine.

In fact, the rotor resistance is determined using the conductivity of bars in the rotor. So, in order to minimize the frequency effect in the general model, the value taken for the stator pulsation, w_{s}, is smaller than its nominal value.

The oscillations of the dynamic response of the general model are due to the slotting effect. Table 3 shows a comparison between the non-linear model response and the response of the general model. We note that the difference between the two results is bigger for the torque than the difference for the currents. This difference can be explained by the fact that the general model accounts the frequency effect.

In Figure 14, we show, for the machine of 45 kW, the torque calculated by the linear model. The difference between the torque value obtained by this model and the Dc level of the general model torque is of 8%.

Initial condition: $[\Phi]_0\,[I]_0$
Calculation step $t + \Delta t$
  Research of $[\Phi]_{t+\Delta t}$:
    First prediction $[\Phi]^0_{t+\Delta t} = [\Phi]_t$
    For i=1,2,....
    While norm $([G]_{t+\Delta t} - [H]^i_{t+\Delta t}\,[\Phi]^i_{t+\Delta t}) \leq$ relative error do
      Calculation of $[\Phi]^{i+1}_{t+\Delta t}$ (Newton Raphson, substitution)
      Research of $[I]^{i+1}_{t+\Delta t}$:
        First prediction $\left[[I]^{i+1}_{t+\Delta t}\right]^0 = [I]^i_{t+\Delta t}$
        For j=1,2,....
        While norm $([\Phi]^{i+1}_{t+\Delta t} - \left[[M]^{i+1}_{t+\Delta t}\right]^j \left[[I]^{i+1}_{t+\Delta t}\right]^j) \leq$ relative error do
          Calculation of $\left[[I]^{i+1}_{t+\Delta t}\right]^{j+1}$ (Newton Raphson, substitution)
          j=j+1
  calculation of the motor torque
  calculation of the motor speed
  $t = t + \Delta t$

Fig. 13. Resolution algorithm of the non-linear electro-mechanical equations.

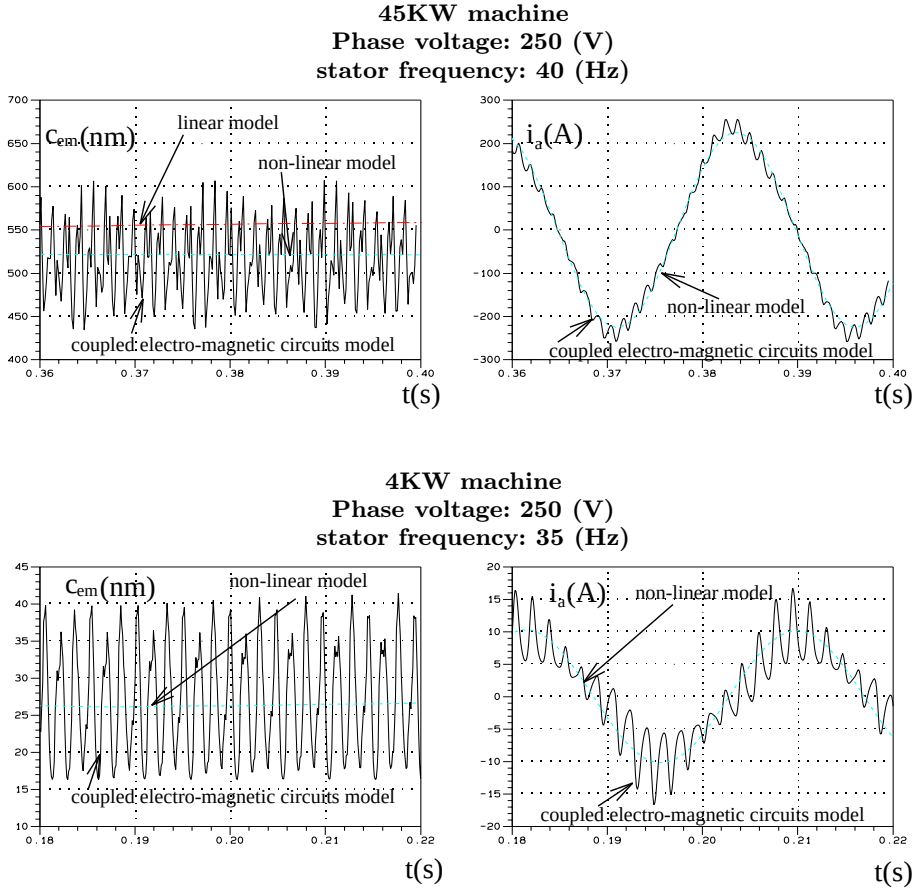

Fig. 14. Dynamic response.

Table 3. Dynamic response results.

45 kW machine	Motor torque (nm) Dc level	Phase one current (A) First harmonic
Non-linear model	516.23	223.34
General model	511.59	223.21
Difference %	0.9	0.058

4kW machine	Motor torque (nm) Dc level	Phase one current (A) First harmonic
Non-linear model	26.26	10.10
General model	26.88	9.90
Difference %	2.31	1.98

7 Conclusion

In this paper we presented an improved non-linear model of the induction machine, based on the Park's two-phase model, which takes in consideration the magnetic state of the machine. The main objective was to determine the flux-current relationships under saturation conditions.

Using $EFCAD$ program, we demonstrated, taking into account the supposed hypothesis, that the magnetic state of an induction machine is determined by the modulus of the magnetising current.

The validated non-linear model only needs the curves of self and mutual cyclic inductances calculated by the module $EFCR$ of $EFCAD$ program.

The most interesting point of our approach is that it does not consider any constrains on the leakage inductances (leakage inductances are included in self inductances).

The approach is validated by comparing its dynamic response with the dynamic response of a general model based on the coupled electro-magnetic equations. The results are very close to the results obtained by this model, in regards to the results obtained from the linear model.

The resolution algorithm of the electro-mechanical equations issued from our model demands a very small calculation time comparing with the calculation time of the general model. This permits to introduce it in the control simulation programs of the induction machine and to improve the classical control laws.

References

1. A.C. Smith, S. Williamson, and J.R. Smith. IEE Elec. Power Appl. **160**, (1990).
2. B. Semail, *Modélisation et réalisation d'un actionneur asynchrone et de sa commande vectorielle*, Ph. D. thesis, LGEP, Paris IV, 1990.
3. D. Bajodeck, *Modèle multi-enroulement de la machine asynchrone*, DEA training, LEEI – INPT, Toulouse, 1994.
4. G. Dhatt, G. Touzot, *Une présentation de la méthode des éléments finis*, edited by S.A. Maloine, 2nd ed. (Oxford, 1984).
5. L. Lesenne, F. Notelet, G. Ségier, *Introduction à l'électrotechnique approfondie* (Technique et Documentation, France, 1981).
6. N. Sadowski, *Modélisation des machines électriques à partir de la résolution des équations du champ en tenant compte du mouvement et du circuit d'alimentation (logiciel $efcad$)*, Ph.D. thesis, LEEI – INPT, Toulouse, 1993.
7. O. Ojo, M. Vipin, I. Bhat, IEEE Trans. Ind. Appl. **30**, 1638 (1994).
8. P. Vas, M. Alakula. IEEE Trans. Energy Conv. **5**, 218 (1990).
9. R.D. Lorenz, D.W. Novotny, IEEE Trans. Ind. Appl. **26** 283 (1990).